Δελτίο της Ελληνικής Γεωλογικής Εταιρίας, τόμος L, σελ. 124-133
Πρακτικά 14ου Διεθνούς Συνεδρίου, Θεσσαλονίκη, Μάιος 2016

Bulletin of the Geological Society of Greece, vol. L, p. 124-133
Proceedings of the 14th International Congress, Thessaloniki, May 2016

DEFORMATION PATTERN IN THE WESTERN NORTH AEGEAN TROUGH: PRELIMINARY RESULTS

Sakellariou D.[1], Rousakis G.[1], Vougioukalakis G.[2], Ioakim Ch.[2], Panagiotopoulos I.[1], Morfis I.[1], Zimianitis E.[2], Athanasoulis K.[2], Tsampouraki-Kraounaki K.[1], Mpardis D.[1] and Karageorgis A.P.[1]

[1]Institute of Oceanography, Hellenic Centre for Marine Research, 19013 Anavyssos, Greece, sakell@hcmr.gr, rousakis@hcmr.gr, jpanagiot@hcmr.gr, gianmor@hcmr.gr, konstantina.ts.kraounaki@gmail.com, nlkrio@gmail.com, ak@hcmr.gr

[2]Institute of Geology and Mineral Exploration, 1st Spirou Louis St., Olympic Village, 13677, Acharnae, Greece, gvoug@igme.gr, ioakim@igme.gr, zimianitis@igme.gr, athanasoulis@igme.gr

Abstract

Preliminary interpretation of swath bathymetry data and seismic profiles acquired during four cruises of "YPOTHER/Aegean Explorations" project aboard R/V Aegaeo provides insights into the fault network, fault kinematics and deformation pattern of the western part of the North Aegean Trough (NAT). The N40°E trending western part of the dextral North Anatolian Fault (NAF) runs along the southern margin of the NAT. Numerous high-angle fault splays initiate from and at low angle to NAF. They run firstly in NE-SW direction and then gradually turn to SE-NW forming an imbricate fault pattern, a nicely developed horsetail structure at the western termination of the NAF. The horsetail pattern deforms the NAT's sedimentary infill forming elongate, curved, uplifting or subsiding tectonic blocks arranged along the fault splays. Instead of the expected transtension, the Western NAT's infill displays dextral shearing and transpression associated with a major stress axis in NW-SE direction. The possible explanation for the transpressional deformation of the Western NAT infill may be related with the change of the trend of NAF from N40°E in the western trough to N70°E east of Lemnos Island.

Keywords: *strike-slip fault, horsetail structure, transtension, transpression, North Anatolian Fault.*

Περίληψη

Πρώτα αποτελέσματα της επεξεργασίας βυθομετρικών δεδομένων και σεισμικών τομών που συλλέχθηκαν στη διάρκεια τεσσάρων πλόων του προγράμματος ΕΣΠΑ "YPOTHER/Aegean Explorations" με το Ω/Κ Αιγαίο παρέχουν νέα στοιχεία για τον τεκτονικό ιστό, την κινηματική των ρηγμάτων και το είδος της παραμόρφωσης στο δυτικό τμήμα της Τάφρου του Βορείου Αιγαίου (NAT). Το δυτικό τμήμα του Ρήγματος Βόρειας Ανατολίας (NAF), με διεύθυνση N40°E, εντοπίζεται κατά μήκος του νότιου περιθωρίου της NAT. Πολυάριθμα δευτερεύοντα ρήγματα με μεγάλη γωνία κλίσης αρχίζουν από το ίχνος του NAF και με μικρή γωνία ως προς αυτό. Η διεύθυνση τους αλλάζει σταδιακά από NE-SW σε SE-NW και δημιουργούν ένα σύνολο επάλληλων και διακλαδιζόμενων, καμπύλων ρηγμάτων, μια καλοσχηματισμένη δομή "ουράς αλόγου" (horsetail structure) στο δυτικό άκρο του NAF. Η δομή αυτή παραμορφώνει την ιζηματογενή ακολουθία της NAT δημιουργώντας επιμήκη, ατρακτοειδούς και καμπύλου

σχήματος, ανυψούμενα και βυθιζόμενα, τεκτονικά μπλοκ. Σε αντίθεση με το αναμενόμενο πλαγιο-εφελκυστικό καθεστώς, το δυτικό τμήμα της ΝΑΤ παραμορφώνεται με διάτμηση και πλαγιο-συμπίεση που συνάδουν με συμπίεση σε διεύθυνση NW-SE. Η πιθανή εξήγηση της παραμόρφωσης αυτής σχετίζεται με την αλλαγή της διεύθυνσης του NAF από N40°E σε N70°E στο ανατολικό τμήμα της ΝΑΤ.
Λέξεις κλειδιά: *ρήγμα οριζόντιας ολίσθησης, δομή "ουράς αλόγου", πλαγιο-εφελκυσμός, πλαγιο-συμπίεση, Ρήγμα Βόρειας Ανατολίας.*

1. Introduction

The northern boundary of the actively deforming Aegean Region to the relatively not-deforming, stable Eurasia continent is marked by the North Aegean Trough (NAT), a complex, almost 300km long depression, ranging from the Pelion Peninsula on the west to the Gulf of Saros on the east. NAT has developed along the westward prolongation of the dextral strike-slip North Anatolian Fault (NAF) (McKenzie, 1970, 1972, 1978; Brunn, 1976; Dewey and Sengör, 1979; Sengör, 1979; Le Pichon and Angelier, 1979, 1981; McKenzie and Jackson, 1983; Taymaz *et al.*, 1991; Armijo *et al.*, 1999). Detailed morphological and morphotectonic analysis of the western part of NAT has been given by Papanikolaou *et al*. (2002). Data on the seismic stratigraphy of NAT's infill indicate up to 6km thick Middle or Late Miocene to present sediments including evaporite-bearing strata, with the thickest deposits located below the Sporadhes Basin (Needham *et al.*, 1973; Jongsma, 1975; Lalechos and Savoyat, 1979; Brooks and Ferentinos, 1980; Lyberis, 1984; Mascle and Martin, 1990).

Systematic and comprehensive interpretation of the fault network in the NAT has been firstly presented by Mascle and Martin (1990) on the basis of low-resolution multi-channel seismic profiles and more recently by Papanikolaou *et al*. (2002, 2006) based on swath bathymetry data and single channel seismic profiles. The steep, southern margin of the Trough has developed along a major fault zone, considered as the westward prolongation of the North Anatolian Fault in the North Aegean Sea through the Saros Gulf. Both the trace of NAF and the axis of the NAT display a dual character in terms of trend: a) N40°E in the western part, Sporadhes Basin, between Pelion Peninsula and Lemnos Island and b) N70°E in the eastern part, east of Lemnos Island and the Saros Gulf (Fig. 1). Mascle and Martin (1990) suggest that the western part of the NAT was created by NW-SE extension in Middle or Late Miocene which may have progressively followed by NE-SW extension along with a transcurrent component due to the dextral movement of the NAF.

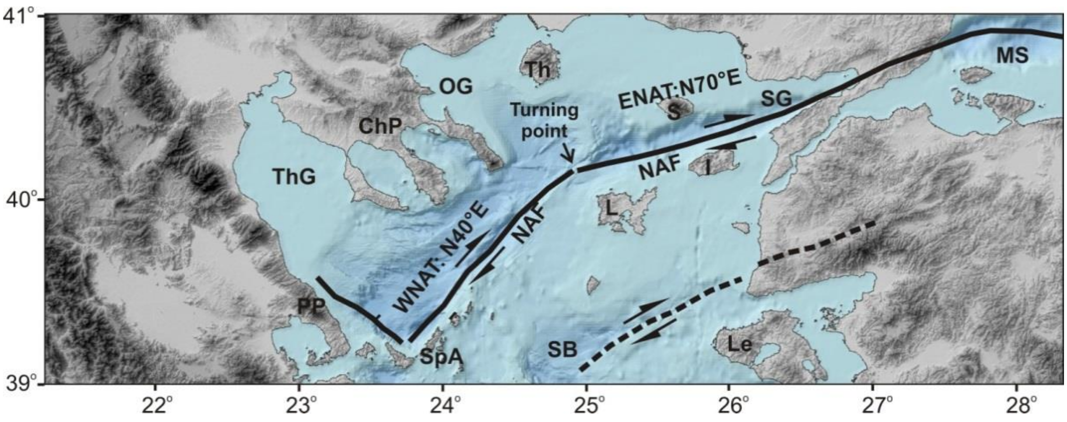

Figure 1 - EMODNET 250m grid DEM of the North Aegean Sea with the western and eastern parts of the North Aegean Trough. ChP: Chalkidiki Peninsula, I: Imvros, L: Lemnos, Le: Lesvos, MS: Marmara Sea, PP: Pelion Peninsula, S: Samothraki, SB: Skyros Basin, SG: Saros Gulf, SpA: Sporadhes Archipelago, Th: Thasos, ThG: Thermaikos Gulf.

GPS measurements over the last decades (Le Pichon *et al*., 1995; Barka and Reilinger, 1997; Reilinger *et al*., 1997, 2000; Kahle *et al*., 2000, McClusky *et al*., 2000, Müller *et al*., 2013) indicate that oblique opening at 30mm/yr across the Sporades Basin is compatible with the cumulative deformation of the basin (Papanikolaou *et al.*, 2002; 2006). Refined analysis and interpretation of previous GPS data by Nyst and Thatcher (2004) suggest that the predicted South Marmara-Eurasia motion across the northern North Anatolian Fault and the North Aegean Trough is 23 mm/yr of almost pure right-lateral strike-slip. Their model requires all relative motion between central and northern Greece to occur across the North Aegean Trough, while GPS velocity gradients across the North Anatolian Trough are high, with 60–70% of Eurasia-South Aegean relative motion occurring there. Building on the previous works as briefly described above, we present new swath bathymetry and seismic profiling data from the western part of the North Aegean Trough, between Pelion and Lemnos Island, we provide new information on the seismic stratigraphy and the fault network and we discuss the deformation pattern of NAT's sedimentary infill.

2. Materials and Methods

Data presented hereafter were collected during four cruises of R/V AEGAEO in the western NAT in 2013, 2014 and 2015, in the framework of the nationally funded "YPOTHER/Aegean Explorations" project, implemented by the Institute of Geology & Mining Exploration (IGME) and the Hellenic Centre for Marine Research (HCMR). Swath bathymetry data were acquired with a 20 kHz SeaBeam 2120 (L3 ELAC Nautic), hull-mounted, multibeam system and were complemented with data acquired in 2000 (Papanikolaou *et al.*, 2002), reprocessed at 25m grid.

An airgun (BOLT) operating with air-chambers of $10in^3$ and $40in^3$ volume, triggered at 4 seconds rate with frequency range between 20 and 400 Hz, was used for the acquisition of single channel seismic profiles. A Sauer Compressor Type WP4351 (J.P. SAUER & SOHN, DE) delivered pressurized air at 2000psi and a SIG streamer, Model 16.48.65, 65m length with 48 hydrophones at 1m spacing was used for the reception of the seismic signal. SB-Logger and SB-Interpreter software (Triton Inc.) was used for the digital acquisition and processing of the profiles. In total, about 420 nautical miles of airgun $40in^3$ and 225 nautical miles of airgun $10in^3$ were acquired across the western NAT and its southern margin respectively.

3. Results

3.1. Seismic Stratigraphy

The seismic source used in this survey provided maximum resolution of about 10 milliseconds and penetration up to about 1.2 to 1.5 seconds two-way travel time below the seafloor at frequency range between 20 and 400Hz. These characteristics allow a fairly detailed study of the seismic stratigraphy of the upper part of the western NAT's sedimentary infill.

Three major, basin wide, seismic stratigraphic units have been distinguished on the basis of their seismic character, separated from each other by two major unconformities (Fig. 3 and 4):

The uppermost seismic unit Q is characterized by a sequence of continuous, parallel, densely spaced, high-amplitude reflectors alternating with low-amplitude, transparent layers. The thickness of Q ranges from 0.1-0.2 seconds in the relatively uplifted parts of the basin to >0.5 seconds in the relatively subsided parts. Maximum thicknesses have been observed below the southwestern part of the western NAT, north of Alonissos Island and east of Skopelos Island and the southern Pelion Peninsula, and in the area southeast of Mount Athos. The seismic character of unit Q with the alternating high- and low-amplitude reflectors indicates continuous sediment deposition during the successive high and low sea-level stages of Quaternary.

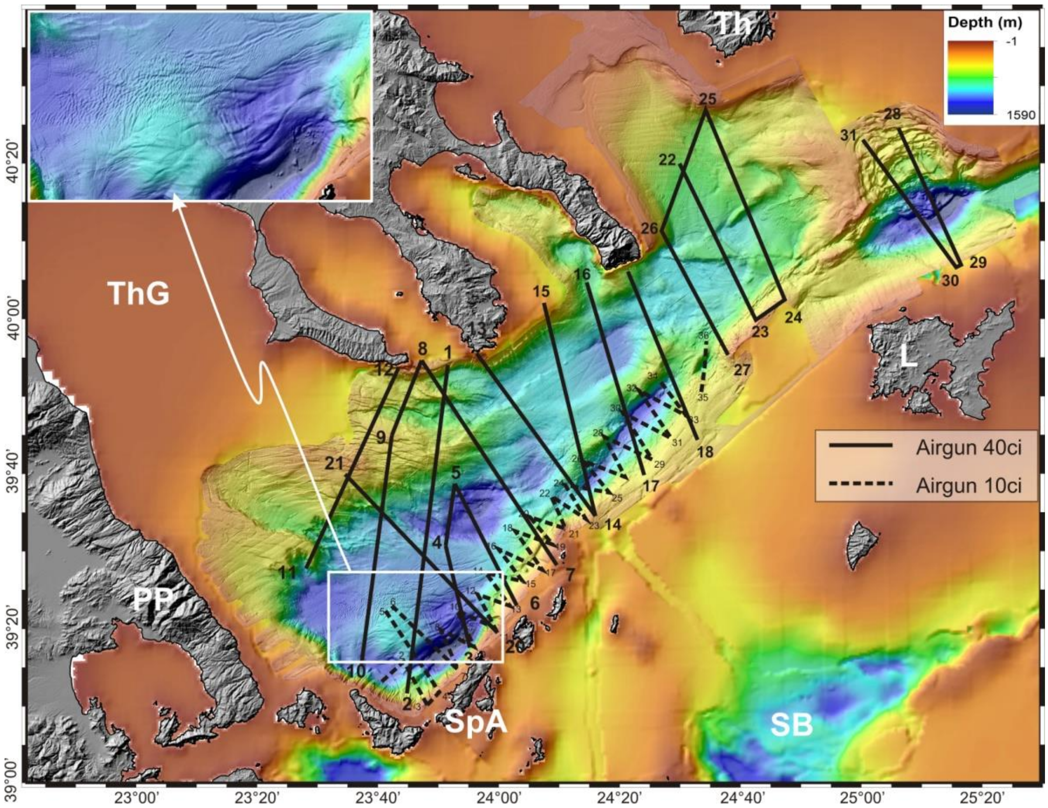

Figure 2 - Seismic profiles and swath bathymetry (25m grid) in the western NAT, EMODNET bathymetry (250m grid, www.emodnet.eu) in the surrounding areas and SRTM90 land topography. Inset map shows detail of the Sporadhes basin's seafloor.

The lower reflectors of unit Q onlap a major unconformity (orange line, Fig. 3 and 4) which marks the top of unit P. The latter displays in general a more transparent acoustic character, with wider spaced, parallel internal reflectors. The transparent acoustic character of unit P becomes dominant in the lower half of it. The thickness of unit P ranges between 0.2-0.3 seconds in the relatively uplifted parts of the basin and >0.5-1.0 seconds in the same areas as above for unit Q. The internal reflectors of unit P onlap a major unconformity (blue line, Fig. 3 and 4) which marks the top of unit M. In agreement with the seismic stratigraphic interpretation given by Mascle and Martin (1990) we consider this unconformity as the top of the Messinian and ascribe a Pliocene age to unit P.

Consequently, unit M represents sediments, including evaporites, deposited in the Messinian and Upper Miocene. The base of unit M has not been imaged with the seismic source used in this survey, thus no information on its thickness can be given. Note that the depocenters of units Q and P occur in the same locations and coincide with the areas of maximum sediment thickness observed by Lyberis (1984). The acoustic basement represents the alpine basement of the area. In the profiles presented here it has been imaged only below the margins of the basin.

3.2. Fault Network

The most striking tectonic element in the western NAT is the westernmost part of the North Anatolian Fault. Detailed mapping by using high resolution swath bathymetry and short seismic lines across the southern margin of NAT revealed over twelve individual segments which all together form the complex fault zone of NAF at its termination. Some of the fault segments overlap with others, they frequently display anastomosing shape and they form structural "highs" and "lows" along the trace of the major fault zone. Very significant cumulative subsidence of NAT in respect to its southern margin

(Sporadhes Arhipelago) of >2km (Papanikolaou *et al.*, 2006) or even >4km as indicated by the seismic data presented here has occurred simultaneously to the dextral horizontal offset. In fact, we observe that maximum subsidence occurs below the southwestern corner of NAT and coincides with the area of maximum sediment thickness accumulated since the Messinian (Fig. 3). The enhanced subsidence north of Alonissos Isl. and east of Skopelos Isl. and Pelion Peninsula (Papanikolaou *et al.*, 2006) is driven by both the SW-NE trending dextral NAF and the NNW-SSE trending, apparently normal faults which mark the western margin of NAT (Fig. 5).

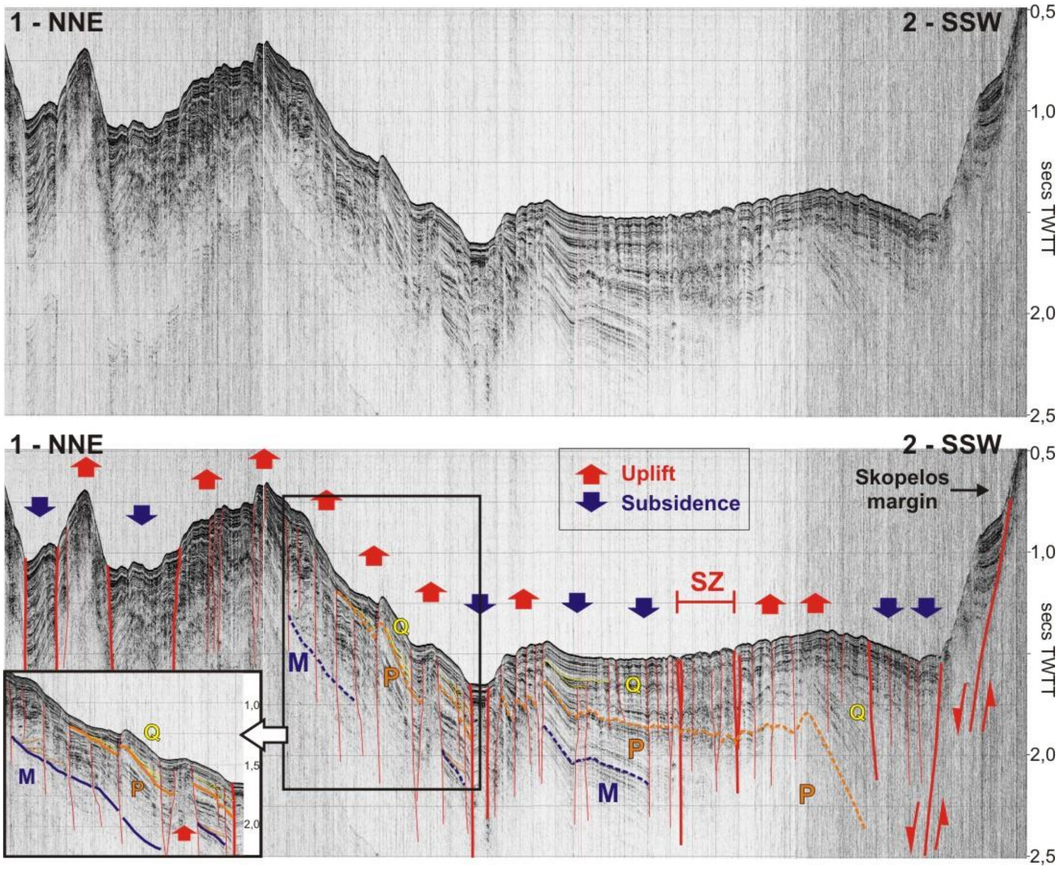

Figure 3 - Airgun 40in^3 seismic profile (Line 1-2, see Fig. 2 for location). Vertical exaggeration X15. Inset: Detail of interpreted profile with two unconformities at the top of M and P. The blue line marks the top of Messinian (M). The orange line marks the top of Pliocene (P). Yellow lines indicate reflectors within Quaternary (Q). SZ: Shear Zone. Red and Blue arrows indicate relative uplift and subsidence of the basin's floor, respectively.

An equally important feature is the numerous, smaller or larger faults and fault splays, which crosscut predominantly the southwestern half of the western NAT (Fig. 3, 4 and 5). Combined analysis of the new swath bathymetry data and the seismic profiles has shown that they originate from the trace of the NAF and are curved: they initially run towards SW, then progressively bend to E-W and finally turn to NW-SE direction, as they enter the Thermaikos Gulf, where they fade out. In the section of the sub-seafloor imaged in the seismic profiles, most of the faults and fault splays are very steep (>60°) or nearly vertical, their sense of vertical motion changes both along strike and with depth, they are closely spaced and form negative or positive flower structures (Fig. 3 and 4). Such a positive flower structure has been imaged by the profile shown in Fig. 4. The profile's section of Fig. 7B of Mascle and Martin (1990) from the same area is given for comparison.

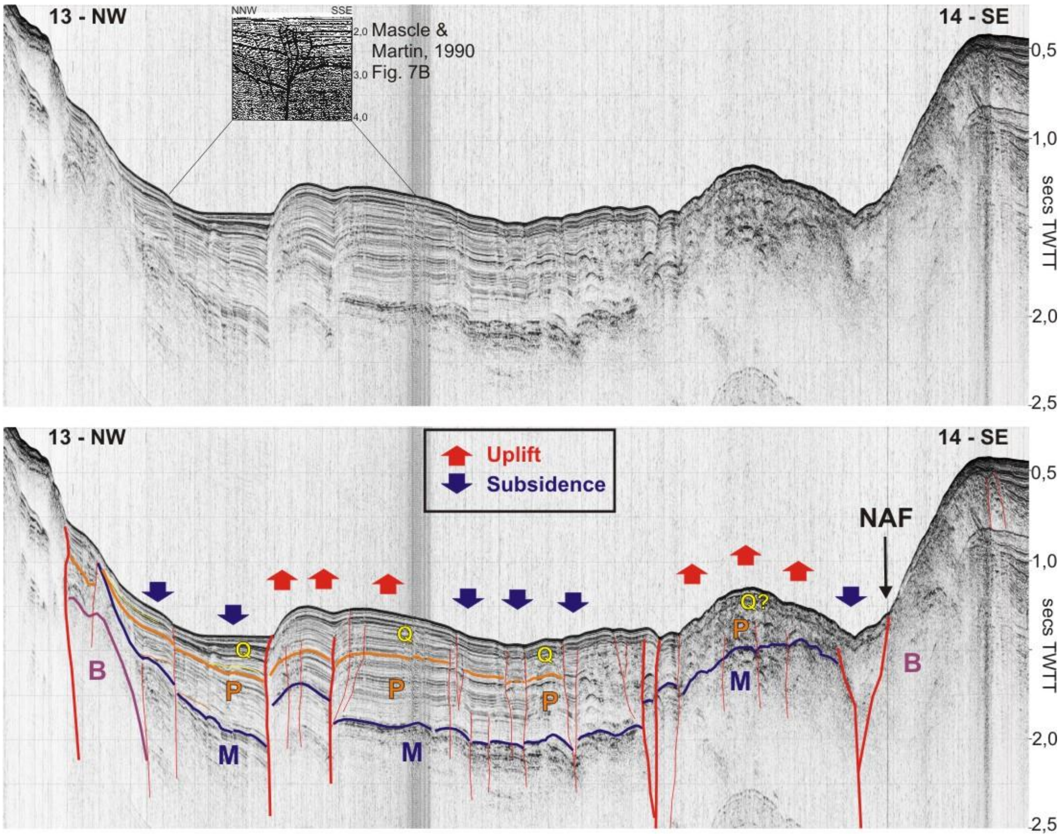

Figure 4 - Airgun 40in^3 seismic profile (Line 13-14, see Fig. 2 for location). Vertical exaggeration X10. The blue line marks the top of Messinian (M). The orange line marks the top of Pliocene (P). Yellow lines indicate reflectors with Quaternary (Q). B: Acoustic / Alpine Basement. Red and Blue arrows indicate relative uplift and subsidence, respectively. Inset profile from Mascle and Martin (1990, Fig. 7B).

At the scale of the basin we observe that the numerous faults and fault splays separate the basin's infill into uplifted and subsided vertical slices (Fig. 3 and 4). In the western half of the survey area (Fig. 3) the basin displays a dual character: the northern half is uplifted forming an anticline-like structure, with the individual slices displaying increasing uplift rate from the flanks to the hinge of the anticline. The southern half is relatively uniformly subsided, though split in vertical slices too. Subsidence increases rapidly south of a distinctive zone of enhanced shearing (SZ in Fig. 3; see also "shear zone" of Papanikolaou *et al*., 2006) which has almost entirely destroyed the seismic stratigraphic texture within it (Fig. 3). In map view (Fig. 2, Fig 5) the shear zone is curved and extends from the western bounding fault (Pelion) to the trace of NAF at the southern margin. The seafloor within this zone is undulating, with the axes of the "anticlines" and "synclines" running SW-NE, oblique to the WNW-ESE trending shear-planes of the shear zone (Inset map in Fig. 2). We interpret this zone as a dextral, intra-basin shear-zone which transfers shear-motion from the southern part of the western (Pelion, Skopelos), NE-facing, predominantly normal, bounding fault to the predominantly dextral strike-slip NAF.

Further east (Fig. 4) the deformation pattern changes within the basin. The northern part displays subsidence, while the southern part has been uplifted, as postulated by both the morphology of the seafloor and the updomed shape of the top of the Messinian (blue line). Uplift and subsidence is again driven by intra-basin faults and faults splays. Figure 6 shows a map of the western NAT with the spatial distribution of uplift and subsidence and their relationship with the tectonic framework.

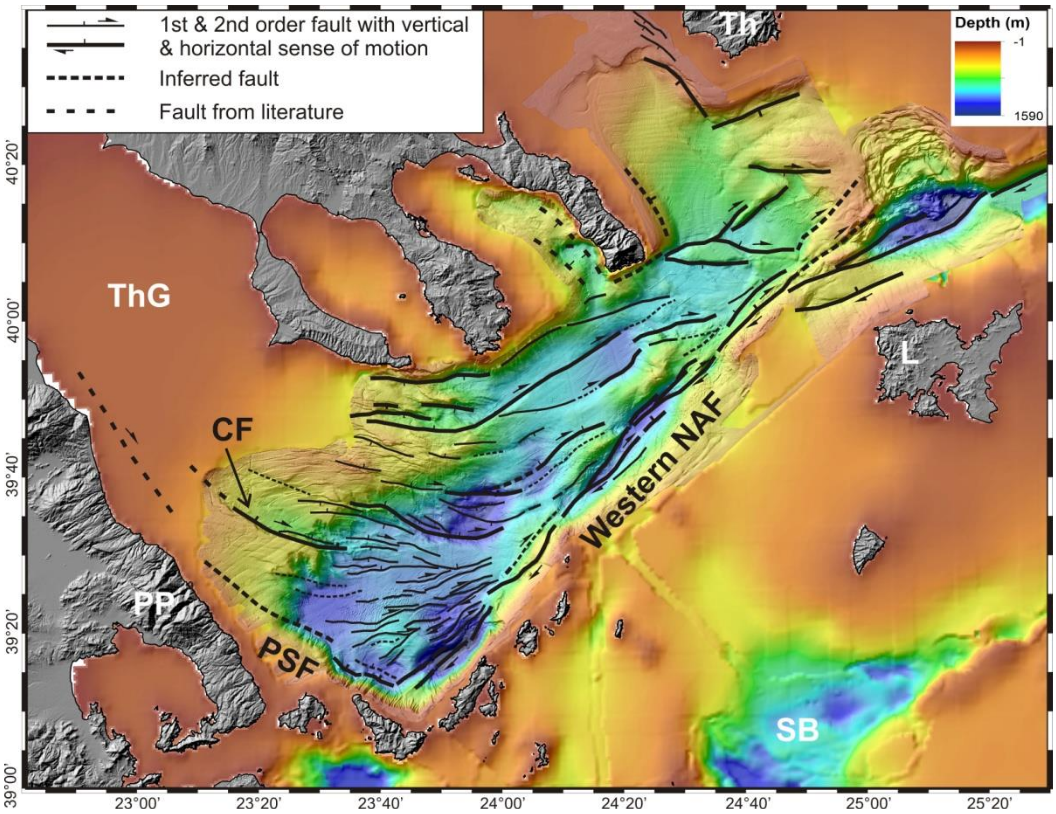

Figure 5 - Fault network in the western North Aegean Trough. NAF: North Anatolian Fault; PSF: Pelion-Skopelos Fault; CF: the "Crustal Fault" studied by Laigle *et al*. (2000).

4. Discussion

We interpret the overall complicate, imbricate fault network observed in the western North Aegean Trough as a right-stepping "horsetail structure" developed at the western termination of the North Anatolian Fault, on the side of the northeastwards moving block.

This interpretation, although partially compatible with the expected geometry and spatial configuration of the faults and fault splays in other, similar, horsetail structures, contradicts to the expected fault-kinematics. Right-stepping horsetail structures are associated with dextral shearing along with oblique normal (extensional) motion along low-angle, listric, imbricate faults and fault splays. In the western NAT the faults and fault splays are steep, while the overall image of the Plio-Quaternary infill presents a rather shear-dominated character along the fault splays and a SW-NE oriented transpression instead of extension, as indicated by the uplifting and subsiding, vertical slices and the overall "folding" at the scale of the basin, as shown on the profile of Fig. 3.

We believe that the discrepancy described above can be explained by considering that the North Anatolian Fault in the Aegean Sea is split into two main segments: an eastern one, running N70°E, and a western one, running N40°E (Fig. 7), with the bending point located north of Lemnos Island. We suggest that the dominant principal stress axis σ1, responsible for the dextral strike-slip motion, trends N65°W - N115°E, at 45° angle in respect to the eastern NAF segment. The "normally expected" prolongation of the latter towards west would follow the white dashed line in Fig. 7. Instead, the western NAF segment runs at 75° in respect to the inferred σ1. This geometrical relationship results in oblique compression towards the western NAF segment.

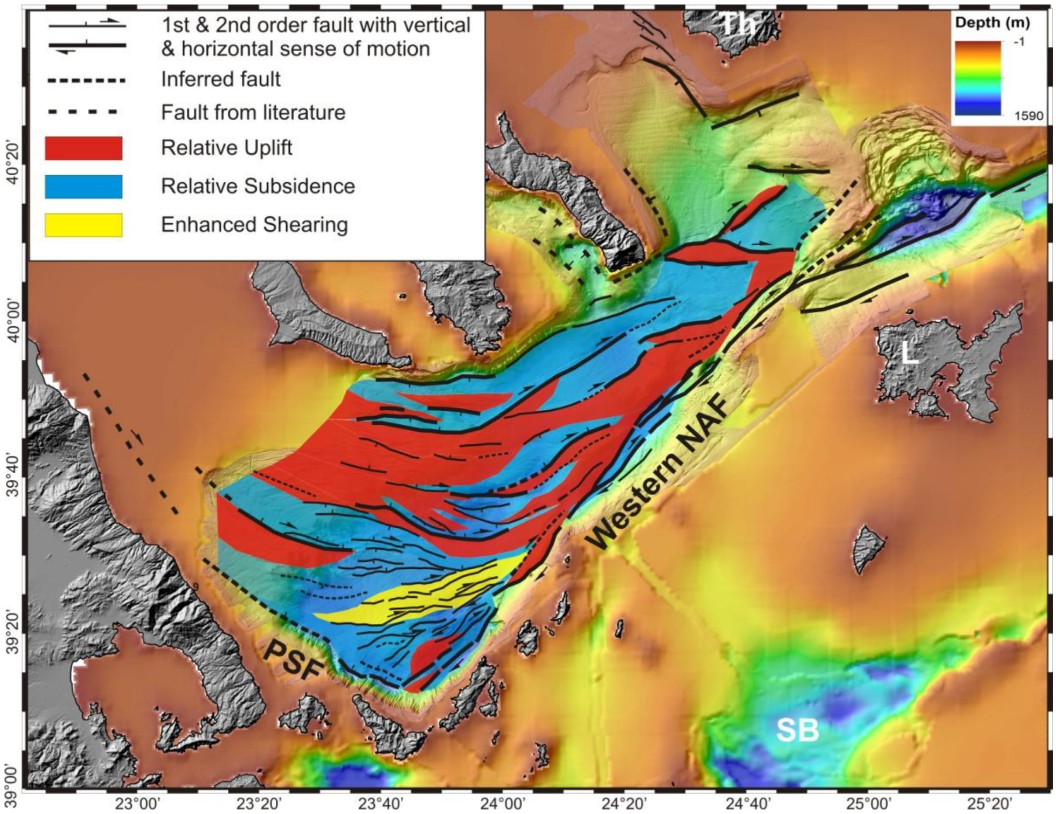

Figure 6 - Fault network and deformation pattern in the western North Aegean Trough. Zones of uplift and subsidence are shown in red and blue colours respectively. The yellow zone indicates a dextral shear zone transferring strain from the NE-facing, Pelion-Skopelos margin to the dextral NAF. Note that maximum subsidence and Plio-Quaternary sediment thickness occurs below the SW corner of the basin, south of the yellow-coloured shearzone.

We note that the western part of NAT has developed within the triangle delineated by the virtual prolongation of the eastern NAF segment (Fig. 7), the NE-facing Pelion-Skopelos Fault and the western NAF segment. Due to the prevailing stress regime and the dextral strike-slip motion the basin is forced to move towards N70°E, away from the Pelion-Skopelos Fault but obliquely towards the N40°E western NAT segment. This kinematic geometry leads to: (i) the enhanced subsidence, observed both in this paper and by Lyberis (1984), below the southwestern corner of NAT, south of the "Shear Zone" (yellow zone in Fig. 6), (ii) the creation of the "horsetail" faults and fault splays, along which the basin infill is split into nearly vertical, curved slices moving towards NE, tending to escape from the "obstacle" posed by the obliquely trending western NAF and (iii) the enhanced transpressional deformation observed in the western NAT.

5. Conclusions

Three seismic stratigraphic units of Quaternary, Pliocene and Messinian / Upper Miocene age, separated from each other by two major unconformities at the top of Pliocene and of Messinian, have been recognized in the upper 1.0-1.5 seconds two-way travel-time below the seafloor of the western North Aegean Trough. The total thickness of the Plio-Quaternary deposits ranges between 0.2-0.3 seconds and >1.5 seconds. Maximum thickness occurs below the southwestern corner of NAT, where the NAF meets the Pelion-Skopelos NE-facing Fault.

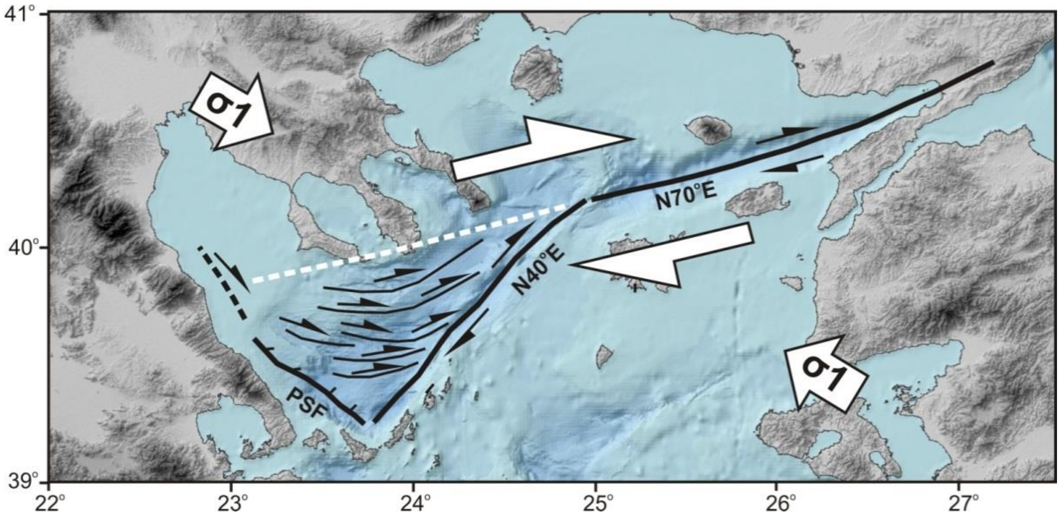

Figure 7 - Tectonic sketch of the North Aegean Trough with the main tectonic elements and the suggested, dominant stress field. The white dashed line marks the virtual westward prolongation of the N70°E trending eastern sector of NAF. Note that the western NAT and the observed horsetail structure have developed within the triangle delineated by the white line, the Pelion-Skopelos Fault (PSF) and the western, N40°E trending sector of NAF.

Numerous high-angle, curved faults and fault splays crosscut the basin's infill, separating it in uplifting and subsiding slices (elongate, curved, tectonic blocks) and forming a nicely developed, right-stepping, horsetail structure at the western termination of NAF. Instead of transtensional deformation accommodated by listric, extensional faults, the western NAT rather displays transpression and shearing along the intra-basinal faults and fault splays.

We explain this discrepancy as the result of the bending of the North Anatolian Fault from N70°E east of Lemnos Island to N40°E along the southern margin of the western NAT. The here proposed N65°W-N115°E directed principal stress axis σ1 is compatible with the dextral strike-slip motion along the eastern, N70°E trending, segment of NAF. The western NAT is being pushed eastwards to collide obliquely with the western, N40°E trending segment of the NAF, undergoes extensive shearing and transpression in a tendency to escape towards northeast. True subsidence and extension is localized at the SW corner of the western NAT, north of the westernmost segments of the NAF, east of the NE-facing Pelion-Skopelos Fault and south of the roughly E-W trending shear zone connecting the two faults.

6. Acknowledgments

The authors are grateful to Captain Theodoros Kanakaris and the crew of R/V AEGAEO for their untiring efforts to ensure the smooth running of the scientific operations during the offshore surveys in the North Aegean Sea. This research is funded by the National Strategic Development Programme ("ESPA").

7. References

Armijo, R., Meyer, B., King, G., Rigo, A. and Papanastassiou, D., 1996. Quaternary evolution of the Corinth rift and its implications for Late Cenozoic evolution of the Aegean, *Geophys. J. Int.*, 126, 11-53.

Billiris, H., Paradissis, D., Veis, G., England, P., Featherstone, W., Parsons, B., Cross, P., Rands, P., Rayson, M., Sellers, P., Ashkenazi, V., Davison, M., Jackson, J. and Ambraseys, N., 1991. Geodetic determination of tectonic deformation in central Greece from 1900 to 1988, *Nature*, 350, 124-129.

Brooks, M. and Ferentinos, G., 1980. Structure and evolution of the Sporades basin of the North Aegean Trough, Northern Aegean Sea, *Tectonophysics*, 68, 15-30.

Clarke, P.J., Davies, R.R., England, P.C., Parsons, B., Billiris, H., Paradissis, D., Veis, G., Cross, P.A., Denys, P.H., Ashkenazi, V., Bingley, R., Kahle, H.G., Muller, M.V. and Briole, P., 1998. Crustal strain in central Greece from repeated GPS measurements in the interval 1989-1997, *Geophys. J. Int*., 135, 195-214.
Davies, R., England, P., Parsons, B., Billiris, H., Paradissis, D. and Veis, G., 1997. Geodetic strain of Greece in the interval 1892-1992, *J. Geophys. Res*., 102, 24,571-24,588.
Dewey, J. and Sengor, A.M.C., 1979. Aegean and surrounding region: Complex multiplate and continuum tectonics in convergent zone, *Geol. Soc. Am. Bull*., 90, 84-92.
Hancock, P.L. and Barka, A.A., 1980. Plio-Pleistocene reversal of displacement on the North Anatolian Fault Zone, *Nature*, 286(5773)5, 91-594.
Jongsma, D., 1975. A Marine Geophysical Study of the Hellenic Arc, Ph.D, Thesis, Cambridge University.
Laigle, M., Hirn, A., Sachpazi, M. and Roussos, N., 2000. North Aegean crustal deformation: An active fault imaged to 10 km depth by reflection seismic data, *Geology*, 28, 71-74.
Lalechos, N. and Savoyat, E., 1979. La sedimentation Neogene dans le Fosse Nord Egeen, 6th Colloquium on the Geology of the Aegean Region, 2, 591-603.
Le Pichon, X. and Angelier, J., 1979. The Hellenic Arc and trench system: A key to the neotectonic evolution of the eastern Mediterranean area, *Tectonophysics*, 60, 1-42.
Le Pichon, X. and Angelier, J., 1981. The Aegean Sea, Philos, *Trans. R. Soc. London*, Ser. A, 300, 357-372.
Le Pichon, X., Chamot-Rooke, N., Lallemant, S., Noomen, R. and Veis, G., 1995. Geodetic determination of the kinematics of central Greece with respect to Europe, *J. Geophys. Res*., 100, 12,675-12,690.
Lyberis, N., 1984. Tectonic evolution of the North Aegean Trough. *In*: The Geological Evolution of the Eastern Mediterranean, *Spec. Publ. Geol. Soc*., 17, 709-725.
McClusky, S., Balassanian, S., Barka, A., Demir, C., Ergintav, S., Georgiev, I., Gurkan, O., Hamburger, M., Hurst, K., Kahle, H., Kastens, K., Kekelidze, G., King, R., Kotzev, V., Lenk, O., Mahmoud, S., Mishin, A., Nadariya, M., Ouzounis, A., Paradissis, D., Peter, Y., Prilepin, M., Reilinger, R., Sanli, I., Seeger, H., Tealeb, A., Toksöz, M.N. and Veis, G., 2000. Global Positioning System constraints on plate kinematics and dynamics in the eastern Mediterranean and Caucasus, *J. Geophys. Res*., 105, 5695-5719.
McKenzie, D.P., 1972. Active tectonics of the Mediterranean region, *Geophys. J. R. Astron. Soc*., 30, 109-185.
McKenzie, D.P., 1978. Active tectonics of the Alpine Himalayan Belt, the Aegean Sea and surrounding regions, *Geophys. J. R. Astron. Soc*., 55, 217-252.
McKenzie, D.P. and Jackson, J.A., 1983. The relationship between strain rates, crustal thickening, paleomagnetism, finite strain and fault movements within a deforming zone, *Earth Planet. Sci. Lett.*, 65, 182-202.
McKenzie, D. and Jackson, J., 1986. A block model of distributed deformation by faulting, *J. Geol. Soc. London*, 143, 349-353.
Mascle, J. and Martin, L., 1990. Shallow structure and recent evolution of the Aegean Sea: A synthesis based on continuous reflection profiles, *Marine Geology*, 94, 271-299.
Müller, M.D., Geiger, A., Kahle, H.G., Veis, G., Billiris, H., Paradissis, D. and Felekis, S., 2013. Velocity and deformation fields in the North Aegean domain, Greece, and implications for fault kinematics, derived from GPS data 1993-2009, *Tectonophysics*, 597-598, 34-49.
Needham, H.D., Le Pichon, X., Melguen, M., Pautot, G., Renard, V., Avedik, F. and Carre, D., 1973. North Aegean sea trough: 1972 Jean Charcot cruise, *Bull. Geol. Soc. Greece*, 10, 152-153.
Nyst, M. and Thatcher, W., 2004. New constraints on the active tectonic deformation of the Aegean, *J. Geoph. Res*., 109, B11406, doi: 10.1029/2003JB002830, 2004.
Papanikolaou, D., Alexandri, M., Nomikou, P. and Ballas, D., 2002. Morphotectonic structure of the western part of the North Aegean Basin based on swath bathymetry, *Marine Geology*, 190, 465-492.
Papanikolaou, D., Alexandri, M. and Nomikou, P., 2006. Active faulting in the north Aegean basin, *Geol. Soc. America*, Sp. Paper 409, 189-209, doi: 10.1130/2006.2409(11).
Sengör, A.M.C., 1979. The North Anatolian transform fault: its age, offset and tectonic significance, *J. Geol. Soc. London*, 136, 269-282.
Taymaz, T., Jackson, J.A. and McKenzie, D., 1991. Active tectonics of the north and central Aegean Sea, *Geophys. J. Int*., 106, 433-490.